

## RESEARCH OUTPUTS / RÉSULTATS DE RECHERCHE

### Nonlinear optical properties in open-shell molecular systems

Nakano, Masayoshi; Champagne, Benoît

*Published in:*

Wiley Interdisciplinary Reviews: Computational Molecular Science

*DOI:*

[10.1002/wcms.1242](https://doi.org/10.1002/wcms.1242)

*Publication date:*

2016

*Document Version*

Publisher's PDF, also known as Version of record

[Link to publication](#)

*Citation for pulished version (HARVARD):*

Nakano, M & Champagne, B 2016, 'Nonlinear optical properties in open-shell molecular systems', *Wiley Interdisciplinary Reviews: Computational Molecular Science*, vol. 6, no. 2, pp. 198-210.

<https://doi.org/10.1002/wcms.1242>

#### General rights

Copyright and moral rights for the publications made accessible in the public portal are retained by the authors and/or other copyright owners and it is a condition of accessing publications that users recognise and abide by the legal requirements associated with these rights.

- Users may download and print one copy of any publication from the public portal for the purpose of private study or research.
- You may not further distribute the material or use it for any profit-making activity or commercial gain
- You may freely distribute the URL identifying the publication in the public portal ?

#### Take down policy

If you believe that this document breaches copyright please contact us providing details, and we will remove access to the work immediately and investigate your claim.



# Nonlinear optical properties in open-shell molecular systems

Masayoshi Nakano<sup>1\*</sup> and Benoît Champagne<sup>2</sup>

For more than 30 years, nonlinear optical (NLO) properties of molecular systems have been actively studied both theoretically and experimentally due to their potential applications in photonics and optoelectronics. Most of the NLO molecular systems are closed-shell species, while recently open-shell molecular species have been theoretically proposed as a new class of NLO systems, which exhibit larger NLO properties than the traditional closed-shell NLO systems. In particular, the third-order NLO property, the second hyperpolarizability  $\gamma$ , was found to be strongly correlated to the diradical character  $y$ , which is a quantum-chemically defined index of effective bond weakness or of electron correlation: the  $\gamma$  values are enhanced in the intermediate  $y$  region as compared to the closed-shell ( $y = 0$ ) and pure open-shell ( $y = 1$ ) domains. This principle has been exemplified by accurate quantum-chemical calculations for polycyclic hydrocarbons including graphene nanoflakes, multinuclear transition-metal complexes, main group compounds, and so on. Subsequently, some of these predictions have been substantiated by experiments, including two-photon absorption. The fundamental mechanism of the  $y$ - $\gamma$  correlation has been explained by using a simple two-site model and the valence configuration interaction method. On the basis of this  $y$ - $\gamma$  principle, several molecular design guidelines for controlling  $\gamma$  have been proposed. They consist in tuning the diradical characters through chemical modifications of realistic open-shell singlet molecules. These results open a new path toward understanding the structure–NLO property relationships and toward realizing a new class of highly efficient NLO materials. © 2016 The Authors. *WIREs Computational Molecular Science* published by John Wiley & Sons, Ltd.

How to cite this article:

*WIREs Comput Mol Sci* 2016, 6:198–210. doi: 10.1002/wcms.1242

## INTRODUCTION

During the past 50 years due to their wide applications in spectroscopy, photonics, optoelectronics, etc., nonlinear optical (NLO) properties have attracted a great deal of attention from experimental and theoretical researchers in many fields (physics,

chemistry, biology, and materials science).<sup>1,2</sup> Nonlinear optics describes various physicochemical phenomena where the properties of light are modified by matter and *vice versa*. These phenomena are caused by intense light sources like with lasers,<sup>1,2</sup> and include (1) frequency mixing, which generates light having frequencies different from those of the incident light such as second-harmonic generation (SHG) and third-harmonic generation (THG), (2) intensity dependent refractive index, leading to light beam self-focusing or defocusing, and (3) multiphoton absorption like two-photon absorption (TPA), where pairs of photons simultaneously excite molecular systems.<sup>1,2</sup> These phenomena are described by the nonlinear polarization terms in the  $\mu = \mu_0 + \alpha$

\*Correspondence to: mnaka@cheng.es.osaka-u.ac.jp

<sup>1</sup>Department of Materials Engineering Science, Graduate School of Engineering Science, Osaka University, Osaka, Japan

<sup>2</sup>Laboratoire de Chimie Théorique, University of Namur, Namur, Belgium

Conflict of interest: The authors have declared no conflicts of interest for this article.

$E + \beta E^2 + \gamma E^3 + \dots$  expansion formula, where  $\mu$  is the dipole moment ( $\mu_0$  is the permanent dipole moment),  $\alpha$  is the polarizability, and  $E$  the electric field amplitude (in this work, we concentrate on the effects of the electric field component of light, whereas magnetic and mixed electric-magnetic effects also exist but are usually weaker). The nonlinear coefficients,  $\beta$  and  $\gamma$ , are referred to as the first and second hyperpolarizabilities, respectively. For example, the SHG and THG phenomena are characterized by real parts of  $\beta$  and  $\gamma$ , whereas TPA is associated with the imaginary part of  $\gamma$ . In order to realize such fascinating applications, molecules and materials exhibiting highly efficient NLO properties are requested together with simple rules to control them. Thus, lots of investigations have been performed to clarify the underlying mechanism of NLO responses and to design molecular and material with targeted NLO responses. In the early studies on the NLO materials, inorganic crystals, e.g., lithium niobate ( $\text{LiNbO}_3$ ) and potassium dihydrogen phosphate ( $\text{KH}_2\text{PO}_4$ ), were employed because they exhibit large SHG effects. Then, since the 1990s,  $\pi$ -electron conjugated organic molecular systems have attracted much attention<sup>1,2</sup> due to their larger optical nonlinearities and faster optical responses as well as feasible molecular design and lower processing cost. Most of these studies have been focused on closed-shell molecular systems and there have been few studies dealing with the NLO properties of open-shell molecular systems before our studies on the spin multiplicity effects on the NLO properties<sup>3</sup> and the diradical character dependences of the NLO properties.<sup>4</sup> In this article, we focus on the latter topics, where the open-shell nature of open-shell singlet systems plays a major role in the control of NLO properties.<sup>5</sup>

Open-shell singlet systems, e.g., diradical systems, have been investigated to understand the chemical bond nature, i.e., its covalent and ionic components in the ground state.<sup>6–8</sup> The simplest examples are the stretched  $\text{H}_2$  and twisted ethylene molecules, and are involved in attractive organic chemical reactions and unique optical transitions.<sup>9</sup> These phenomena have been rationalized in terms of the diradical character ( $y$ ;  $0 \leq y \leq 1$ ), a quantum-chemically well-defined index.  $y$  defines both an effective bond weakness (chemical view) and the localization versus delocalization of the electrons or electron correlation (physical view).<sup>5,10</sup> In this article, we introduce the diradical character dependence of the third-order NLO properties, e.g., the second hyperpolarizability  $\gamma$  at the molecular scale, for a two-site model based on the perturbative formula including excitation energies and transition moments.

From this theoretical result, we describe the correlation between  $y$  and  $\gamma$ , referred to as ‘ $y$ - $\gamma$  correlation,’ and state the following NLO-design principle: ‘ $\gamma$  values of systems with the intermediate diradical character ( $y \sim 0.5$ ) are enhanced as compared to those of closed-shell ( $y = 0$ ) and pure open-shell ( $y = 1$ ) singlet systems.’<sup>11</sup> Then, we summarize theoretical investigations on a wide variety of model and real molecular systems with intermediate diradical characters that lead to control schemes of the diradical character through chemical modification and physical perturbation.<sup>5,12–23</sup> We also introduce extensions of the  $y$ - $\gamma$  correlation, e.g., for multiradical systems going beyond diradicals,<sup>24–26</sup> dynamic (frequency-dependent) hyperpolarizabilities,<sup>27,28</sup> asymmetric open-shell singlet systems,<sup>23,29</sup> and spin state dependence.<sup>13,26</sup> From the experimental side, several real open-shell singlet molecular systems have recently been synthesized and have been found to exhibit large TPA-cross sections<sup>30–35</sup> and large THG properties<sup>36,37</sup> (typical third-order NLO properties), the facts of which substantiate the ‘ $y$ - $\gamma$  correlation’ principle. It is thus expected that ‘open-shell singlet NLO systems’ surpass the conventional closed-shell NLO systems, and also exhibit multifunctionalities, e.g., optical and magnetic properties, as well as a high controllability via chemical and physical modifications.<sup>5</sup>

## OPEN-SHELL NATURE AND EXCITATION ENERGIES/ PROPERTIES

### Two-Site Model in the Valence Configuration Interaction Scheme

In order to reveal the relationship between excitation energies/properties, which determine the hyperpolarizabilities and open-shell nature, i.e., diradical character, we consider the simplest two-site model  $\text{A}^\bullet\text{--B}^\bullet$  with two electrons in two active orbitals in the valence configuration interaction (VCI) scheme.<sup>8,11</sup> Using bonding and antibonding molecular orbitals (referred to as  $g$  and  $u$ , respectively), the localized natural orbitals (LNOs; referred to as  $a$  and  $b$ ) are expressed as  $a \equiv (g+u)/\sqrt{2}$  and  $b \equiv (g-u)/\sqrt{2}$ , which are nearly localized on one site (A or B). For  $M_S$  (the  $z$ -component of spin angular momentum) = 0, we define two neutral ( $|a\bar{b}\rangle$ ,  $|b\bar{a}\rangle$ ) and two ionic ( $|la\bar{a}\rangle$ ,  $|b\bar{b}\rangle$ ) determinants, where the upper-bar indicates the  $\beta$  spin, while non-bar does the  $\alpha$  spin. The electronic Hamiltonian matrix for the two-site model is described using several physical parameters, namely,

effective Coulomb repulsion  $U(\equiv U_{aa} - U_{ab})$  (the difference between on-site and intersite Coulomb integrals), direct exchange integral  $K_{ab}(\equiv \langle a\bar{b} | 1/r_{12} | b\bar{a} \rangle)$ , and transfer integral  $t_{ab}(\equiv \langle a | f | b \rangle)$ , where  $f$  indicates the Fock operator in the LNO basis).<sup>11</sup> By diagonalizing the electronic Hamiltonian matrix, we obtain four electronic states including three singlet states and one triplet state (see Figure 1), i.e., an essentially neutral lowest-energy singlet state of g symmetry  $|g\rangle = \kappa(|a\bar{b}\rangle + |b\bar{a}\rangle) + \eta(|a\bar{a}\rangle + |b\bar{b}\rangle) = \xi|g\bar{g}\rangle - \zeta|u\bar{u}\rangle$  (ground state, with energy  $E_g$ ;  $\kappa > \eta > 0$ ), a pure ionic singlet state with u symmetry  $|k\rangle = (|a\bar{a}\rangle - |b\bar{b}\rangle)/\sqrt{2} = (|g\bar{u}\rangle + |u\bar{g}\rangle)/\sqrt{2}$  (first excited state with energy  $E_k$ ), an essentially ionic singlet state of g symmetry  $|f\rangle = -\eta(|a\bar{b}\rangle + |b\bar{a}\rangle) + \kappa(|a\bar{a}\rangle + |b\bar{b}\rangle) = \zeta|g\bar{g}\rangle + \xi|u\bar{u}\rangle$  (second excited state with energy  $E_f$ ;  $\kappa > \eta > 0$ ), and a neutral triplet state  $|T\rangle = (|a\bar{b}\rangle - |b\bar{a}\rangle)/\sqrt{2} = (|g\bar{u}\rangle - |u\bar{g}\rangle)/\sqrt{2}$  (with energy  $E_T$ ). Here,  $\xi = \kappa + \eta$  and  $\zeta = \kappa - \eta$  are the functions of  $t_{ab}$  and  $U$ , respectively. The Hartree–Fock (HF) ground state (in the mean-field approximation, i.e., in the limit of no electron correlation) is given by  $|g^{HF}\rangle = |g\bar{g}\rangle$ , so that  $\kappa = \eta = 1$ , which corresponds to equal weights for the neutral (covalent) and ionic components. As increasing the electron correlation, the neutral component increases as compared to the ionic one, and finally the ionic component vanishes [ $(\kappa, \eta) = (1/\sqrt{2}, 0)$  or  $(\xi, \zeta) = (1/\sqrt{2}, 1/\sqrt{2})$ ] at the strong correlation limit. In other words,  $\zeta$  increases from 0 to  $1/\sqrt{2}$ , which corresponds to the variation from the stable bond to the bond dissociation limit, so that we can define the diradical character ( $y$ ) as  $y = 2\zeta^2$  [0 (closed-shell)  $\leq y \leq 1$  (pure-diradical)].<sup>10,38</sup>

Owing to the states symmetry, there are only two nonzero transition moments,  $\mu_{gk} = \sqrt{2}\eta R_{BA}$  (between states g and k) and  $\mu_{kf} = \sqrt{2}\kappa R_{BA}$  (between states k and f), where  $R_{BA} \equiv (b|r_1|b) - (a|r_1|a)$  indicates the effective distance between the unpaired electrons.

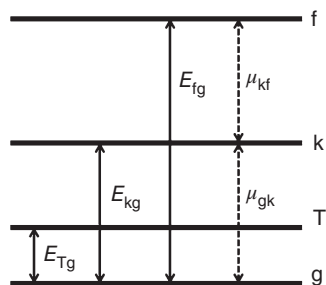


**FIGURE 1** | Singlet three states {g, k, f} and a triplet state {T} together with excitation energies and transition moments of the two-site diradical model with two electrons in two orbitals.

The effective exchange interaction  $J(\equiv (E_g - E_T)/2)$ , which is a function of  $(t_{ab}, U, K_{ab})$ ,<sup>11</sup> describes, within Heisenberg model,<sup>39</sup> the ground state magnetic interaction, where negative/positive  $J$  indicates a singlet/triplet (antiferromagnetic/ferromagnetic) ground state. For the following discussion, we introduce the dimensionless physical quantities:  $r_t \equiv |t_{ab}|/U$  ( $\geq 0$ ),  $r_K \equiv 2K_{ab}/U$  ( $\geq 0$ ), and  $r_f \equiv 2J/U$ . As  $|t_{ab}|$  and  $U$  indicate the easiness and difficulty of electron transfer between the A and B sites, respectively,  $r_t$  represents the degree of electron delocalization over A and B, and  $r_t^{-1}$  the degree of electron localization (electron correlation).  $r_K$  is expressed by, e.g.,  $\langle a\bar{b} | H | b\bar{a} \rangle / U$  or  $\langle a\bar{a} | H | b\bar{b} \rangle / U$ , so that  $r_K$  is proportional to the overlap between  $a$  and  $b$ . The (dimensionless) state energies depend linearly on  $r_K$  ( $\geq 0$ ), with stabilization of the k and T states by an  $r_K$  amount and a destabilization by the same amount for the g and f singlet states. This originates from the relative phase between the LNO  $\{|a\bar{b}\rangle, |b\bar{a}\rangle\}$  in the neutral determinants and  $\{|a\bar{a}\rangle, |b\bar{b}\rangle\}$  in the ionic determinants.

In order to clarify the physical and chemical meanings of  $y$ , it is expressed as a function of these physical quantities:

$$y \equiv 2\zeta^2 = 1 - \frac{4|t_{ab}|}{\sqrt{U^2 + 16t_{ab}^2}} = 1 - \frac{1}{\sqrt{1 + (4r_t)^{-2}}} \quad (1)$$

showing that it is the function of  $r_t^{-1}$  (electron correlation). Indeed,  $y$  increases with  $r_t^{-1}$  as shown in Figure 2: from the delocalization ( $y \rightarrow 0$ ) to the localization ( $y \rightarrow 1$ ) limit, with an electron on each site for the latter. In the present model,  $y$  is also expressed by the occupation number of the lowest unoccupied natural orbital (LUNO),  $n_{LUNO}$ . As  $n_{LUNO} = 2 - n_{HONO}$  and  $q \equiv 1 - y = (n_{HONO} - n_{LUNO})/2$  means an ‘effective bond order’ because  $n_{HONO}$  and  $n_{LUNO}$  are the numbers of electrons in bonding and antibonding orbitals, respectively. From these considerations, the diradical character  $y$  represents electron correlation in the physical sense and an effective bond order in the chemical sense.

The dimensionless excitation energies ( $E_{ig}^{DL}$ ,  $i = k, f$ ) and transition moments squared  $[(\mu_{ij}^{DL})^2, i, j = g, k, f]$  are expressed as a function of the effective bond order  $q(=1 - y)$  by<sup>11</sup>

$$E_{kg}^{DL} \equiv \frac{E_k - E_g}{U} = \frac{1}{2} \left( 1 - 2r_K + \frac{1}{\sqrt{1 - q^2}} \right),$$

$$E_{fg}^{DL} \equiv \frac{E_f - E_g}{U} = \frac{1}{\sqrt{1-q^2}} \quad (2a)$$

$$(\mu_{gk}^{DL})^2 \equiv \left( \frac{\mu_{gk}}{R_{BA}} \right)^2 = \frac{1 - \sqrt{1-q^2}}{2}, \quad (\mu_{kf}^{DL})^2 \equiv \left( \frac{\mu_{kf}}{R_{BA}} \right)^2 = \frac{1 + \sqrt{1-q^2}}{2} \quad (2b)$$

The diradical character dependences of these quantities are shown in Figure 3 for  $r_K = 0$ , which is approximately satisfied for most systems with a singlet ground state. As  $r_K$  is included only in  $E_{kg}^{DL}$ , which originates in the contributions of  $+K_{ab}$  and  $-K_{ab}$  to the energies of the ground (g) and the first excited (k) states, respectively, due to the phase features of their wavefunctions,  $E_{kg}^{DL}$  is reduced by  $r_K$  for any  $y$  value. In the small  $y$  region,  $E_{kg}^{DL}$  decreases

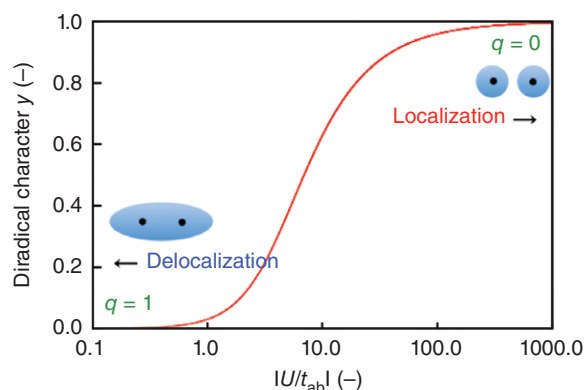


**FIGURE 2** | Diradical character  $y$  versus  $|U/t_{ab}|$ . Effective bond order  $q = 1 - y$  is also shown at delocalization ( $y = 0$ ) and localization ( $y = 1$ ) limits.

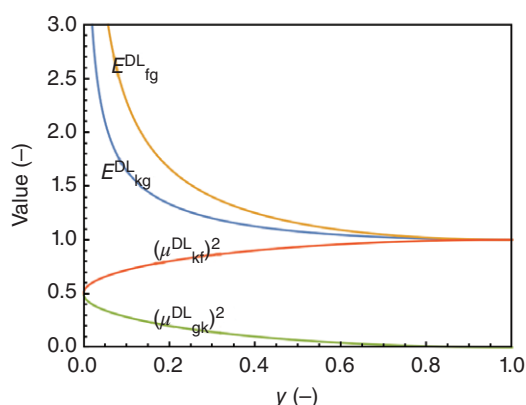


**FIGURE 3** | Diradical character dependences of dimensionless excitation energies ( $E_{kg}^{DL}$  and  $E_{fg}^{DL}$ ), squared transition moments ( $(\mu_{gk}^{DL})^2$  and  $(\mu_{kf}^{DL})^2$ ).

more rapidly with  $y$  than  $E_{fg}^{DL}$ , but they converge toward the same stationary value ( $E_{kg}^{DL} = E_{fg}^{DL} = 1$ ). Note that in the case of a finite  $r_K$ ,  $E_{kg}^{DL}$  converges to  $1 - r_K$ . This diradical character dependence of the DL excitation energies originates from the relative decrease of the transfer integral  $|t_{ab}|$  as compared to  $U$ , which destabilizes (stabilizes) the g (f) state, while it does not affect the k state. Concerning the squared DL transition moments,  $(\mu_{gk}^{DL})^2$  and  $(\mu_{kf}^{DL})^2$  are identical at  $y = 0$  but they monotonically decrease to 0 or increase toward 1 with increasing  $y$ , respectively. These variations stem from the decrease (increase) of the ionic component of state g (f) against state u keeping a pure ionic nature, as a function of  $y$ . One should also emphasize that (1) the excitation energies do not only depend on  $y$  (or  $q$ ) but also on the amplitude of  $U$ , so that  $E_{kg}$  decreases with  $U$  (for a fixed  $t_{ab}$ ) until a minimum and then it increases and that (2) the transition moments squared are proportional to the square of  $R_{BA}$ , which corresponds approximately to system size when the radical sites are well separated.

## Diradical Character Dependence of the Second Hyperpolarizability

Within perturbation theory, the second hyperpolarizability  $\gamma$  is expressed by a sum-over-state (SOS) formula,<sup>1,2</sup> involving the excitation energies, transition moments, and dipole moment differences (Box 1). For the present two-site model in the static limit, this formula leads to the dimensionless second hyperpolarizability  $\gamma^{DL}$  by using Eqs (2(a) and (b)):<sup>11</sup>

$$\gamma^{DL} \equiv \frac{\gamma}{(R_{BA}^4/U^3)} = - \frac{8(1-y)^4}{\left\{ 1 + \sqrt{1-(1-y)^2} \right\}^2 \left\{ 1 - 2r_K + \frac{1}{\sqrt{1-(1-y)^2}} \right\}^3} + \frac{4(1-y)^2}{\left\{ 1 - 2r_K + \frac{1}{\sqrt{1-(1-y)^2}} \right\}^2 \left\{ \frac{1}{\sqrt{1-(1-y)^2}} \right\}} \quad (3)$$

where the first and second terms on the right-hand side correspond to  $\gamma^{II\ DL}$  and  $\gamma^{III-2\ DL}$ , respectively. The variations as a function of  $y$  of these terms as well as of the total  $\gamma^{DL}$  are shown in Figure 4(a) for  $r_K = 0$ .  $\gamma^{DL}$  displays a bell-shape variation with a maximum value at  $y \approx 0.359$ : systems with



## BOX 1

## DIRADICAL CHARACTER AND FUNCTIONALITY

The diradical character  $y$  is not an observable, but a quantum-chemically well-defined index describing the ground state. For two-site two-electron model systems, in the physical sense,  $y$  has the meaning of a degree of localization of the electrons on each site, i.e., of electron correlation, while, in the chemical sense,  $1 - y$  indicates the degree of bond strength or bond order between the two radical sites. Namely, the diradical character is a fundamental index for describing the electronic structure of ground and excited states. It has been shown that an intermediate diradical character makes the electronic state very sensitive to external physical perturbations and chemical modifications, the feature of which implies that systems with intermediate diradical character are functional molecular systems.

intermediate diradical character exhibit larger  $\gamma^{\text{DL}}$  than closed-shell ( $y = 0$ ) and pure diradical ( $y = 1$ ) systems.<sup>11</sup> This bell-shape behavior originates from the dominating  $\gamma^{\text{III-2 DL}}$  term, which takes a maximum ( $\sim 0.243$ ) at  $y \approx 0.306$ , that is caused by the rapid decreases of  $(E_{\text{kg}}^{\text{DL}})^2 E_{\text{fg}}^{\text{DL}}$  and  $(\mu_{\text{gk}}^{\text{DL}})^2 (\mu_{\text{kf}}^{\text{DL}})^2$  as  $y \rightarrow 1$  (Figure 4(b)). The variations of  $\gamma^{\text{DL}}$  as a function of  $y$  and  $r_K$  are shown in Figure 4(c), where the blue curve indicates  $r_f = 0$  and the lower and upper regions of this curve correspond to singlet and triplet ground states, respectively. For small  $r_K$ ,  $\gamma^{\text{DL}}$  in the intermediate  $y$  region (B) is larger than that in the (nearly) closed-shell region (A). Then, upon increasing  $r_K$ ,  $\gamma^{\text{DL}}$  further increases and the maximum  $\gamma^{\text{DL}}$  moves toward larger  $y$  values. The (C) region corresponds to triplet ground state but its singlet excited state with intermediate  $y$  value gives the largest  $\gamma^{\text{DL}}$  values in the examined ( $y, r_K$ ) region. In addition, the region (D) characterized by small  $y$  ( $< \sim 0.4$ ) and large  $r_K$  ( $> \sim 0.8$ ) values provides negative  $\gamma^{\text{DL}}$  values of large amplitudes. Besides the traditional NLO systems (closed-shell region A), we have now found several real molecular systems belonging to region B (open-shell singlet NLO systems) while we have proposed several design guidelines for region B. They are described in this article. Investigating regions C and D is also interesting because molecular magnets may be candidates for these regions. Finally, as

seen from Eq. (3),  $\gamma$  also depends on  $R_{\text{BA}}^4/U^3$ , i.e., it increases proportionally to the fourth power of the effective diradical distance and to the third power of  $U^{-1}$ .

Asymmetric systems form another type of open-shell singlet systems. By employing the asymmetric two-site diradical model, we have described the evolution of  $\gamma^{\text{DL}}$  as a function of  $y_s$ ,  $r_K$ , and  $r_b$ ,<sup>29</sup> where  $y_s$  is the pseudo-diradical character and  $r_b$  indicates the core Hamiltonian difference,  $(h_{bb} - h_{aa})/U$  (set positive), i.e., the ionization energy difference between A and B (referred to as asymmetry). It is found that asymmetric open-shell singlet molecular systems exhibit remarkable enhancements of the local maximum  $\gamma^{\text{DL}}$  amplitudes as compared to the corresponding closed-shell asymmetric systems and symmetric diradical systems with similar diradical character. Similarly, the amplitudes of the first hyperpolarizability  $\beta$  (which varies as a function of  $r_b$ ) are magnified in the intermediate/large  $y_s$  region with respect to the closed-shell region.<sup>29</sup> From these results, asymmetric open-shell singlet systems appear as candidates for building second- and third-order NLO materials, which outstrip those of the traditional closed-shell and symmetric open-shell singlet systems.

## METHODOLOGY

Calculations to sample the  $y - \gamma$  correlation have been performed at different levels of approximation. The reliability of lower-level methods on model compounds has been assessed in comparison to high-level *ab initio* calculations. The latter encompass Full CI and PNOF5 calculations on model hydrogen chains<sup>40,41</sup> as well as unrestricted Coupled Cluster method with singles, doubles, and a perturbative estimate of the triples [UCCSD(T)], spin-flip (SF) CI, and approximate spin-projected unrestricted Møller-Plesset perturbation theory [APUMP $n$ ,  $n = 2-4$ ], that have been employed to study compounds like *p*-quinodimethane (PQM).<sup>4,41-43</sup> Figure 6(a) shows the resonance structure of the latter,<sup>5</sup> where the quinoid and benzenoid forms correspond to the closed-shell and pure open-shell (diradical) states, respectively. Its diradical character was artificially varied over the 0.15–0.7 window by stretching the external CC bond (Figure 6(b)). Results on stretched H<sub>2</sub> demonstrate how close are the Full CI (=CISD = CCSD) and PNOF5 values (Figure 5(a)). Comparisons between UCCSD(T) and other levels of approximation are illustrated in Figure 5(b) and (c). Their analysis has substantiated the adoption of density

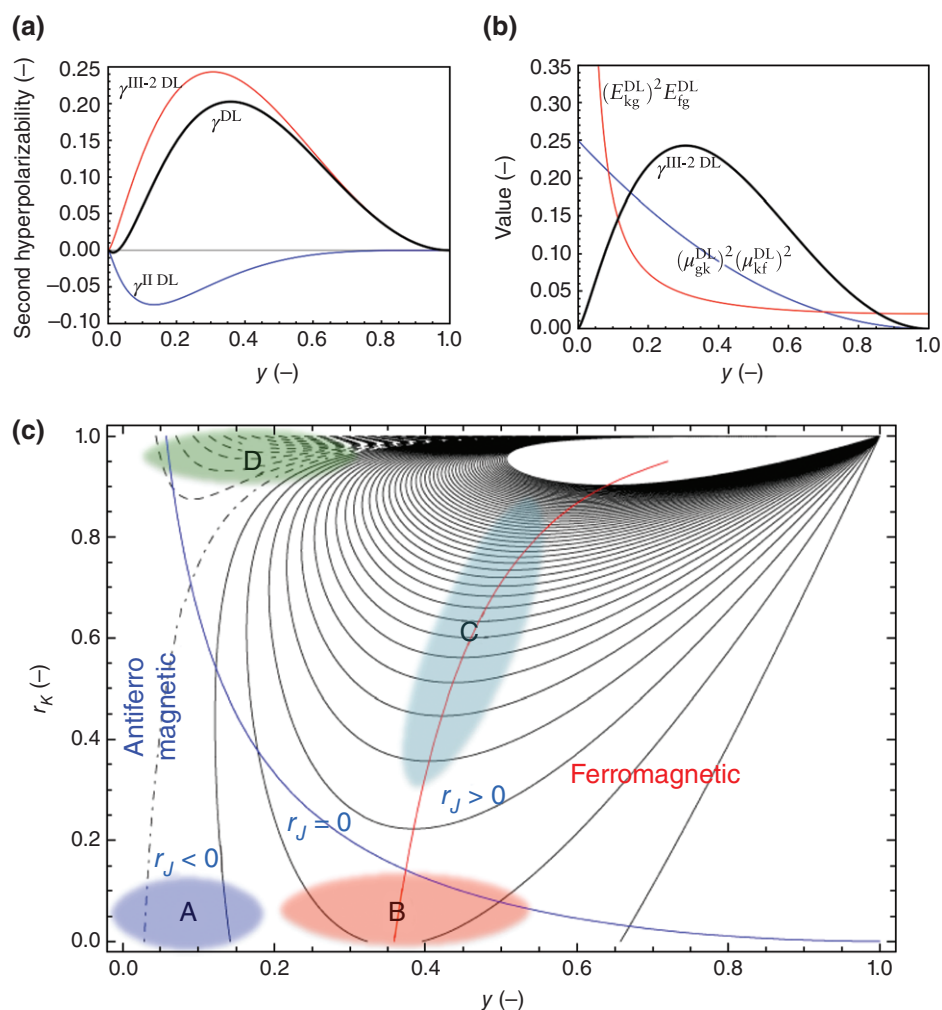


**FIGURE 4** | Variations of second hyperpolarizabilities,  $\gamma^{\text{DL}}$ ,  $\gamma^{\text{II DL}}$ , and  $\gamma^{\text{III-2 DL}}$ , as a function of diradical character ( $\gamma$ ) in the case of  $r_K = 0$  (a),  $\gamma$  dependences of  $\gamma^{\text{III-2 DL}}$ ,  $(\mu_{\text{gk}}^{\text{DL}})^2 (\mu_{\text{kf}}^{\text{DL}})^2$ , and  $(E_{\text{kg}}^{\text{DL}})^2 E_{\text{fg}}^{\text{DL}}$  in the case of  $r_K = 0$  (b), and contours of  $\gamma^{\text{DL}}$  ( $-5.0 \leq \gamma^{\text{DL}} < 5.0$ , interval = 0.1) on the plane ( $\gamma, r_K$ ), where solid, dotted, and dashed black lines indicate positive, negative, and zero lines of  $\gamma^{\text{DL}}$ , respectively (c). In (c), the red line represents the ridge line connecting the ( $\gamma, r_K$ ) points giving maximum  $\gamma^{\text{DL}}$  values. The blue curve indicates  $r_J = 0$  and the lower and upper regions of this curve represent the singlet (antiferromagnetic) and triplet (ferromagnetic) ground states, respectively. Region A and B–D represent closed-shell (traditional NLO systems) and open-shell (theoretically predicted systems) regions, respectively.

functional theory (DFT) to investigate structure–property relationships in larger systems such as phenalenyl derivatives. In the first studies, the BHandH-LYP functional was employed,<sup>4</sup> while, later on, long-range corrected exchange–correlation functionals have been used (more specifically the LC-BLYP functional with a range-separated parameter  $\mu = 0.33$  for organic molecules,<sup>44</sup> whereas for bimetallic systems, larger  $\mu$  values are requested<sup>17</sup>). Approximate spin-projected spin-unrestricted DFT, ASP-LC-UBLYP, was also employed and shown to be reliable, using  $\mu = 0.47$  for PQM (Figure 5(c)).<sup>43</sup>

For this broad range of methods,  $\gamma$  was evaluated using the finite-field procedure, as the fourth-

order derivative of the energy with respect to the electric field. Analyses have been carried out for an adequate choice of the field amplitudes.<sup>45,46</sup> Results were analyzed in terms of the  $\gamma$  density,<sup>47</sup> highlighting the compounds moieties that contribute most to  $\gamma$ . These were related to the odd electron density as well as, in a less rigorous though mostly equivalent way, to the spin density. Basis set effects have also been investigated on several compounds, starting with valence double- $\zeta$ +polarization basis sets and adding a few sets of diffuse functions. In the case of PQM, at the UCCSD(T) level, the 6-31+G(d) basis set overestimates the aug-cc-pVDZ value ( $\gamma = 150 \times 10^3$  a.u.) by 12% while the 6-31G(d)+p

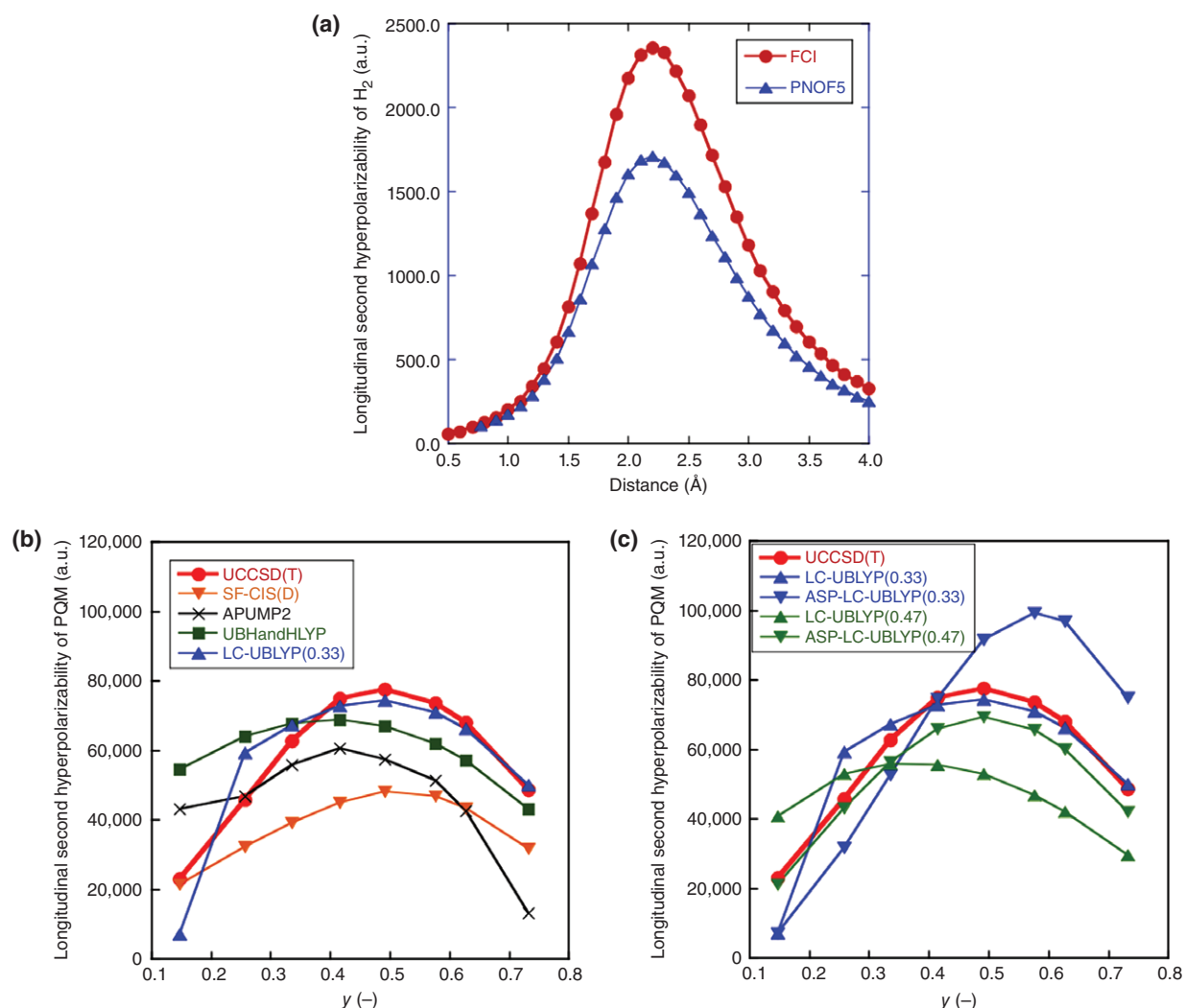


**FIGURE 5** |  $\gamma$  values of model compounds as determined at different levels of approximation. (a) stretched H<sub>2</sub> molecule (aug-cc-pVDZ basis set); (b, c) *p*-quinodimethane with different diradical characters (6-31G(d)+*p* basis set).

basis set performs even better (99%). On the other hand, the 6-31G(d) basis set, which lacks diffuse functions, underestimates  $\gamma$  by about 40%. Still, although these diffuse functions play a non-negligible role on  $\gamma$  of small systems, their impact is more limited on large systems, like graphene nanoflakes (GNFs) and IDPL. For the latter, it was indeed found that the difference between the 6-31G(d) and 6-31G+*p*  $\gamma$  values, evaluated at the HF level, is only about 10%.<sup>12</sup>

## DESIGN GUIDELINES OF OPEN-SHELL SINGLET NLO MOLECULAR SYSTEMS

On the basis of the  $\gamma$  –  $\gamma$  correlation, we expect the molecules with intermediate diradical character to be

superior to the traditional closed-shell conjugated NLO molecules. As shown above for PQM one of the most simple design rules for realizing such stable diradicaloids consists in tuning the quinoid–benzenoid resonance structure (Figure 6(b)). Indeed, the longitudinal component of  $\gamma$  displays a bell-shape variation as a function of  $\gamma$ , where the maximum  $\gamma$  is obtained around  $\gamma = 0.5$ <sup>4</sup> (Figure 5(b)). Still, real PQM has a small diradical character  $\gamma = 0.146$ , as determined at the spin-projected unrestricted Hartree–Fock (PUHF)/6-31G\*+*p* level, tuning the molecular architectures and chemical compositions can lead to intermediate  $\gamma$  values. For example, two phenalenyl rings, each of which bringing an unpaired electron, connected by a condensed-ring conjugated linker provide thermally stable diradicaloids. Figure 7 shows phenalenyl diradicaloids 1(*n*) of



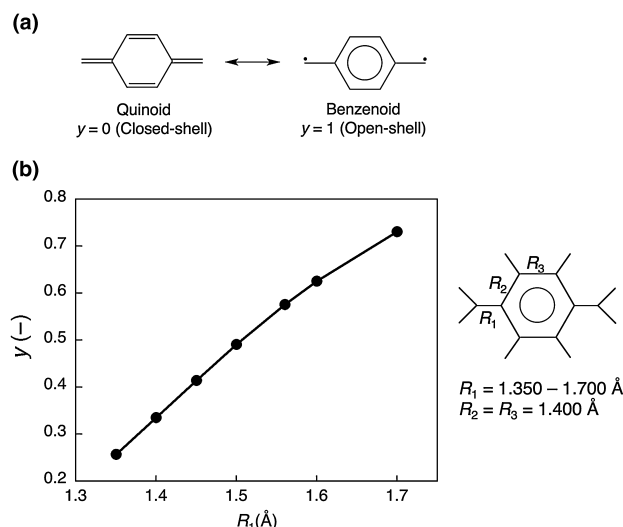


**FIGURE 6** | Resonance structures [quinoid (closed-shell) and benzenoid (open-shell)] of *p*-quinodimethane model (a) and dependence of the diradical character ( $\gamma$ ) as a function of the length of the exo-cyclic carbon–carbon bonds ( $R_1$ ) from 1.350 to 1.700 Å (b) under the bond-length constraint of  $R_2 = R_3 = 1.4$  Å. Note that the equilibrium geometry ( $R_1 = 1.351$ ,  $R_2 = 1.460$ ,  $R_3 = 1.346$  Å, optimized by the RB3LYP/6-311G(d)) gives the lowest diradical character ( $\gamma = 0.146$ ).

different size ( $n = 1$ –3), having  $\gamma = 0.770$ , 0.854, and 0.91, respectively, as well as closed-shell analogue **2** ( $\gamma = 0.0$ ).<sup>12,42</sup> In contrast to **2**, **1**( $n$ ) includes quinoid–benzenoid forms in their resonance structures, which explains the nonzero  $\gamma$  value. Then, increasing the central fused-ring linker increases the aromaticity and therefore the  $\gamma$  value. Thus, although they are of similar size, **1**(1) has a longitudinal  $\gamma$  (that, for simplicity, will be called  $\gamma$ ) value that is about one-order magnitude larger than that of **2**. Then, the monotonous increase of  $\gamma$  with  $n$  originates from the size effect ( $\gamma \propto R_{\text{BA}}^4$ ) in addition to the  $\gamma$  dependence of dimensionless  $\gamma$  (see Eq. (3)). Similarly, **3** (*as*-IDPL) has a nearly pure diradical character (0.923) due to the large aromaticity of the central ring, so that  $\gamma$  of **3** is significantly smaller than that of **1**(1) (IDPL). Such control scheme of the open-shell character through tuning the relative contribution of the quinoid–benzenoid resonance forms is also valid for GNFs **4**–**6** (Figure 7). In these systems, on the basis of Clar's sextet rule,<sup>48</sup> the dominant resonance structures have the most disjoint aromatic  $\pi$ -sextets, i.e., benzene-like moieties so that the multiradical resonance structures are stabilized by their aromaticity. This multiradical nature can be characterized by

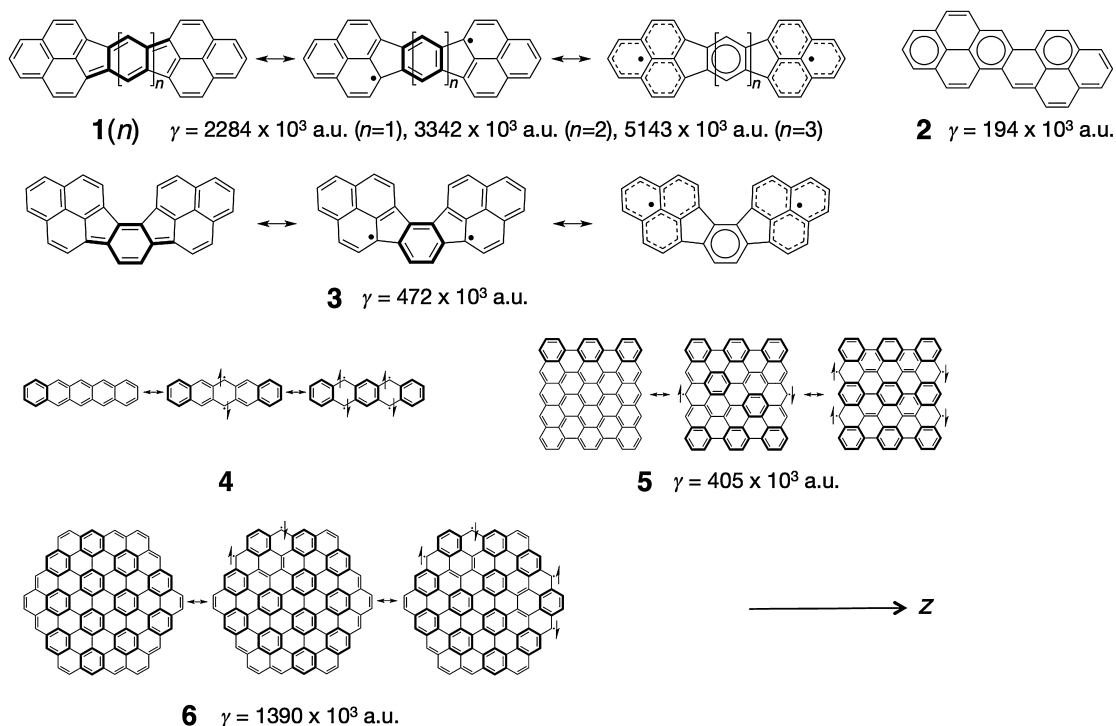


**FIGURE 7** | Resonance structures for open-shell singlet molecules including diphenalenyl compounds (**1**( $n$ ), **3**), oligoacenes (**4**), rectangular graphene nanoflake (GNF) (**5**), and hexagonal GNF (**6**), as well as a closed-shell analogue **2** for **1**(1). The  $\gamma$  ( $\gamma_{\text{zzzz}}$ ) values are calculated using the UBHandHLYP/6-31G (d) method.

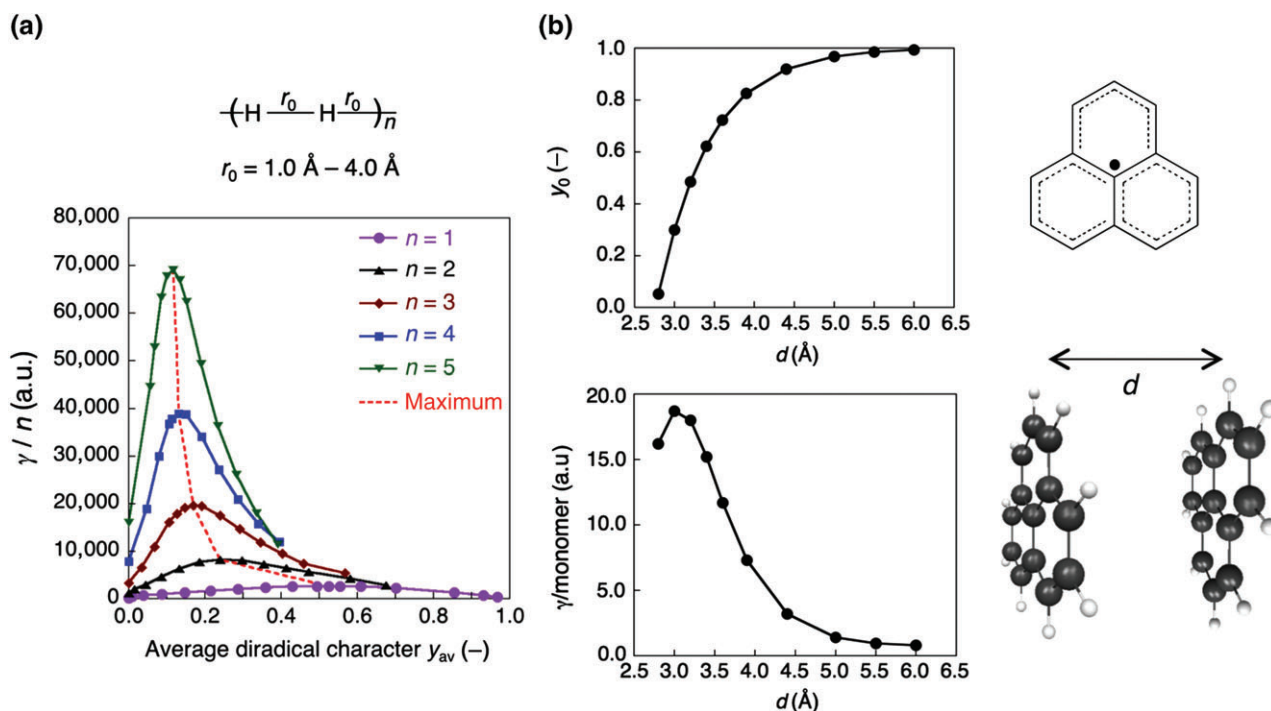


**FIGURE 8** | (a) Dependence of longitudinal  $\gamma/n$  as a function of  $y_{av}$  of regular  $H_{2n}$  chains ( $n = 1-5$ ) calculated by the UCCSD(T)/(6)-31(+) +G(\*) method, where the dotted line represents the displacement of the maximum  $\gamma/n$  value; (b) Dependences of diradical character  $y_0$  and  $\gamma/\text{monomer}$  (in the stacking direction) on the intermolecular distance  $d$  for the  $\pi$ - $\pi$  stacked phenalenyl dimer model.

using multiple diradical characters  $y_i$  ( $i = 0, 1, \dots$ ), which are defined by the LUNO+ $i$  occupation numbers.<sup>10,47</sup> As a result, zigzag-edged GNFs have open-shell nature, while armchair-edged analogues have closed-shell nature.<sup>14,47</sup> In these GNFs, the  $\gamma$ - $\gamma$  correlation is satisfied, provided their sizes are similar.

As multiradical systems, open-shell singlet oligomers and aggregates exhibit further enhancement of their NLO properties and interesting dependences on their multiple diradical characters.<sup>24-26,49</sup> Studies on one-dimensional (1D) hydrogen chain models with different interatomic distances, which realize a wide range of average diradical characters  $y_{av}$ , show that, for different chain lengths, these systems exhibit bell-shape  $y_{av}$ - $\gamma$  variations, and that the maximum  $\gamma/n$  increases with chain length, while the average diradical character ( $y_{av \text{ max}}$ ) giving the maximum  $\gamma/n$  values decreases (Figure 8(a)). Then, the regular multiradical linear chains with small average diradical character exhibit not only larger  $\gamma/n$  amplitudes than closed-shell chains but also significant chain-length dependence, demonstrating the advantage of multiradical linear chains. Going from model to real systems, for 1D  $\pi$ - $\pi$  stacked phenalenyl radical aggregates (Figure 8(b)), the multiple diradical character strongly depends on the intermolecular distance, e.g., for a dimer close to equilibrium stacking

distance, its  $\gamma$  is intermediate and its  $\gamma$  (in the stacking direction) is maximized. The  $\gamma/\text{monomer}$  exhibits about a 30-fold enhancement as compared to the isolated phenalenyl monomer.<sup>50</sup> This suggests that in such pancake bonding the equilibrium distance is an optimum compromise between localization and delocalization of the radical electron pairs. As going from the dimer (diradical) to the tetramer (tetraradical), the  $\gamma$  enhancement ratio increases nonlinearly with the aggregate size, whereas switching from the singlet to the highest (quintet) spin state causes a remarkable reduction of  $\gamma$  by a factor of  $\sim 50$ .<sup>50</sup> Furthermore, switching from the neutral (tetraradical) to the dicationic (diradical) state in the tetramer causes a significant enhancement of  $\gamma$  by a factor of  $\sim 13$ .<sup>50</sup> These results demonstrate that these aggregates composed of radical monomers are potential candidates for a new class of open-shell NLO systems with enhanced third-order NLO properties, which can be switched by changing the spin multiplicity.

## CONCLUSION

The theoretical origin of the third-order NLO responses of open-shell singlet systems is unraveled by using the VCI method, which highlights the

relationships between the excitation energies/properties and the open-shell (diradical) character. Systems with intermediate diradical characters are shown to exhibit larger second hyperpolarizabilities  $\gamma$  than closed-shell and pure diradical systems, giving birth to a new class of highly efficient NLO systems. The diradical character has both physical and chemical meanings, i.e., it describes the degree of electron correlation and the effective bond weakness in the ground state and, qualitatively, it can be predicted based on the resonance structures. Therefore, design rules toward efficient open-shell NLO systems can be constructed for various types of molecular systems, e.g.,  $\pi$ -conjugated condensed-ring molecules described by both quinoid and benzenoid resonance structures, transition-metal—metal bonded systems, and open-shell singlet supramolecular systems. Asymmetric open-shell systems constitute another class of NLO systems, which exhibit further enhancement of  $\gamma$  as compared to symmetric open-shell singlet

analogues. This asymmetry can be introduced by physical perturbation (external electric fields) and/or chemical modifications (donor/acceptor substitutions).<sup>23,29</sup> These guidelines can be extended to other NLO properties like the first hyperpolarizabilities  $\beta$  in the case of asymmetric systems,<sup>29</sup> as well as to frequency-dependent and/or resonant NLO properties.<sup>27,28</sup> Another extension is based on the drastic change of  $\gamma$  by changing the spin multiplicity: the  $\gamma$  values of intermediate diradical systems are significantly reduced by switching from the singlet to the triplet states due to Pauli repulsion/localization effects.<sup>3,13</sup> This behavior is also interesting from the viewpoint of multifunctional NLO systems, where the NLO and magnetic properties can be mutually controlled by applying magnetic fields. In summary, the quest for realistic (stable) open-shell NLO molecular systems and the investigation of design rules based on the diradical character is a fertile research field of materials science and engineering.

## ACKNOWLEDGMENTS

This work was supported by Grant-in-Aid for Scientific Research (A) (No. 25248007) from Japan Society for the Promotion of Science (JSPS), a Grant-in-Aid for Scientific Research on Innovative Areas “Stimuli-Responsive Chemical Species” (No. A24109002a), “ $\pi$ -System Figuration” (15H00999), “Photosynergetics” (A26107004a), MEXT, a Grant-in-Aid for Bilateral Programs Joint Research Projects (JSPS—F.R.S.-FNRS), the Strategic Programs for Innovative Research (SPIRE), MEXT, and the Computational Materials Science Initiative (CMSI), Japan. This study was also financially supported by BELSPO (IUAP 7/05), the Francqui Foundation, and the University of Namur. Theoretical calculations are partly performed using Research Centre for Computational Science, Okazaki, Japan.

## FURTHER READING

- Lambert C. Towards polycyclic aromatic hydrocarbons with a singlet open-shell ground state. *Angew Chem Int Ed* 2011, 50:1756–1758.
- Sun Z, Wu J. Open-shell polycyclic aromatic hydrocarbons. *J. Mater. Chem.* 2012, 22:4151–4160.
- Sun Z, Zeng Z, Wu J. Zethrenes, extended  $\pi$ -quinodimethanes, and periacenes with a singlet biradical ground state. *Acc Chem Res* 2014, 47:2582–2591.
- Kamada K, Ohta K, Shimizu A, Kubo T, Kishi R, Takahashi H, Botek E, Champagne B, Nakano M. Singlet diradical character from experiment. *J. Phys. Chem. Lett.* 2010, 1:937–940.
- Minami T, Nakano M. Diradical character view of singlet fission. *J. Phys. Chem. Lett.* 2012, 3:145–150.
- Minami T, Ito S, Nakano M. Signature of singlet open-shell character on the optically allowed singlet excitation energy and singlet-triplet energy gap. *J. Phys. Chem. A* 2013, 117:2000–2006.
- Breher F. Stretching bonds in main group element compounds—borderlines between biradicals and closed-shell species. *Coord Chem Rev* 2007, 251:1007–1043.
- Nakano M, Champagne B. Theoretical design of open-shell singlet molecular systems for nonlinear optics. *J Phys Chem Lett* 2015, 6:3236–3256.

## REFERENCES

1. Nalwa HS, Miyata S, eds. *Nonlinear Optics of Organic Molecules and Polymers*. Boca Raton, FL: CRC Press; 1997.
2. Papadopoulos MG, Sadlej AJ, Leszczynski J, eds. *Nonlinear Optical Properties of Matter—From Molecules to Condensed Phases*. Dordrecht: Springer; 2006.
3. Nakano M, Nitta T, Yamaguchi K, Champagne B, Botek E. Spin multiplicity effects on the second hyperpolarizability of an open-shell neutral  $\pi$ -Conjugated system. *J Phys Chem A* 2004, 108:4105–4111.
4. Nakano M, Kishi R, Nitta T, Kubo T, Nakasuji K, Kamada K, Ohta S, Botek E, Champagne B. Second hyperpolarizability ( $\gamma$ ) of singlet diradical systems: dependence of  $\gamma$  on the diradical character. *J Phys Chem A* 2005, 109:885–891.
5. Nakano M. *Excitation Energies and Properties of Open-Shell Singlet Molecules: Applications to a New Class of Molecules for Nonlinear Optics and Singlet Fission*. Heidelberg: Springer; 2014.
6. Salem L, Rowland C. The electronic properties of diradicals. *Angew Chem Int Ed* 1972, 11:92–111.
7. Borden WT, ed. *Diradicals*. New York: Wiley; 1982.
8. Bonačić-Koutecký V, Koutecký J, Michl J. Neutral and charged biradicals, zwitterions, funnels in  $S_1$ , and proton translocation: their role in photochemistry, photo-physics, and vision. *Angew Chem Int Ed* 1987, 26:170–189.
9. Abe M. Diradicals. *Chem Rev* 2013, 113:7011–7088.
10. Yamaguchi K. Instability in chemical bonds. In: Carbo R, Klobukowski M, eds. *Self-Consistent Field: Theory and Applications*. Amsterdam: Elsevier; 1990, 727–828.
11. Nakano M, Kishi R, Ohta S, Takahashi H, Kubo T, Kamada K, Ohta K, Botek E, Champagne B. Relationship between third-order nonlinear optical properties and magnetic interactions in open-shell systems: a new paradigm for nonlinear optics. *Phys Rev Lett* 2007, 99:033001–1–4.
12. Nakano M, Kubo T, Kamada K, Ohta K, Kishi R, Ohta S, Nakagawa N, Takahashi H, Furukawa S, Morita Y, et al. Second hyperpolarizabilities of polycyclic aromatic hydrocarbons involving phenalenyl radical units. *Chem Phys Lett* 2006, 418:142–147.
13. Ohta S, Nakano M, Kubo T, Kamada K, Ohta K, Kishi R, Nakagawa N, Champagne B, Botek E, Takebe A, et al. Theoretical study on the second hyperpolarizabilities of phenalenyl radical systems involving acetylene and vinylene linkers: diradical character and spin multiplicity dependences. *J Phys Chem A* 2007, 111:3633–3641.
14. Nakano M, Nagai H, Fukui H, Yoneda K, Kishi R, Takahashi H, Shimizu A, Kubo T, Kamada K, Ohta K, et al. Theoretical study of third-order nonlinear optical properties in square nanographenes with open-shell singlet ground states. *Chem Phys Lett* 2008, 467:120–125.
15. Yoneda K, Nakano M, Kishi R, Takahashi H, Shimizu A, Kubo T, Kamada K, Ohta K, Champagne B, Botek E. Third-order nonlinear optical properties of trigonal, rhombic and bow-tie graphene nanoflakes with strong structural dependence of diradical character. *Chem Phys Lett* 2009, 480:278–283.
16. Yoneda K, Nakano M, Inoue Y, Inui T, Fukuda K, Shigeta Y, Kubo T, Champagne B. Impact of antidot structure on the multiradical characters, aromaticities and third-order nonlinear optical properties of hexagonal graphene nanoflakes. *J Phys Chem C* 2012, 116:17787–17795.
17. Fukui H, Inoue Y, Yamada T, Ito S, Shigeta Y, Kishi R, Champagne B, Nakano M. Enhancement of the third-order nonlinear optical properties in open-shell singlet transition-metal dinuclear systems: effects of the group, of the period, and of the charge of the metal atom. *J Phys Chem A* 2012, 116:5501–5509.
18. Kishi R, Dennis M, Fukuda K, Murata Y, Morita K, Uenaka H, Nakano M. Theoretical study on the electronic structure and third-order nonlinear optical properties of open-shell quinoidal oligothiophenes. *J Phys Chem C* 2013, 117:21498–21508.
19. Matsui H, Fukuda K, Hirosaki Y, Takamuku S, Champagne B, Nakano M. Theoretical study on the diradical characters and third-order nonlinear optical properties of cyclic thiazyl diradical compounds. *Chem Phys Lett* 2013, 585:112–116.
20. Kishi R, Murata Y, Saito M, Morita K, Abe M, Nakano M. Theoretical study on diradical characters and nonlinear optical properties of 1,3-diradical compounds. *J Phys Chem A* 2014, 118:10837–10848.
21. Matsui H, Fukuda K, Takamuku S, Sekiguchi A, Nakano M. Theoretical study on the relationship between diradical character and second hyperpolarizabilities of four-membered-ring diradicals involving heavy main group elements. *Chem-Eur J* 2015, 21:2157–2164.
22. Okuno K, Shigeta Y, Kishi R, Nakano M. Photochromic switching of diradical character: design of efficient nonlinear optical switches. *J Phys Chem Lett* 2013, 4:2418–2422.
23. Nakano M, Minami T, Yoneda K, Muhammad S, Kishi R, Shigeta Y, Kubo T, Rougier L, Champagne B, Kamada K, et al. Giant enhancement of the second hyperpolarizabilities of open-shell singlet polyaromatic diphenalenyl diradicaloids by an external electric field and donor-acceptor substitution. *J Phys Chem Lett* 2011, 2:1094–1098.

24. Nakano M, Takebe A, Kishi R, Ohta S, Nate M, Kubo T, Kamada K, Ohta K, Champagne B, Botek E, et al. Second hyperpolarizabilities ( $\gamma$ ) of open-shell singlet one-dimensional systems: intersite interaction effects on the average diradical character and size dependences of  $\gamma$ . *Chem Phys Lett* 2006, 432:473–479.
25. Nagai H, Nakano M, Yoneda K, Kishi R, Takahashi H, Shimizu A, Kubo T, Kamada K, Ohta K, Botek E, et al. Signature of multiradical character in second hyperpolarizabilities of rectangular graphene nanoflakes. *Chem Phys Lett* 2010, 489:212–218.
26. Motomura S, Nakano M, Fukui H, Yoneda K, Kubo T, Carion R, Champagne B. Size dependences of the diradical character and the second hyperpolarizabilities in dicyclopenta-fused acenes: relationships with their aromaticity/antiaromaticity. *Phys Chem Chem Phys* 2011, 13:20575–20583.
27. Nakano M, Yoneda K, Kishi R, Takahashi H, Kubo T, Kamada K, Ohta K, Botek E, Champagne B. Remarkable two-photon absorption in open-shell singlet systems. *J Chem Phys* 2009, 131:114316–1–7.
28. Nakano M, Champagne B. Diradical character dependence of third-harmonic generation spectra in open-shell singlet systems. *Theor Chem Acc* 2015, 134:23–1–9.
29. Nakano M, Champagne B. Diradical character dependences of the first and second hyperpolarizabilities of asymmetric open-shell singlet systems. *J Chem Phys* 2013, 138:244306–1–13.
30. Kamada K, Ohta K, Kubo T, Shimizu A, Morita Y, Nakasuji K, Kishi R, Ohta S, Furukawa S, Takahashi H, et al. Strong two-photon absorption of singlet diradical hydrocarbons. *Angew Chem Int Ed* 2007, 46:3544–3546.
31. Zeng Z, Sung YM, Bao N, Tan D, Lee R, Zafra JL, Lee BS, Ishida M, Ding J, Navarrete JTL, et al. Stable tetrabenzo-chichibabin's hydrocarbons: tunable ground state and unusual transition between their closed-shell and open-shell resonance forms. *J Am Chem Soc* 2012, 134:14513–14525.
32. Li Y, Heng W-K, Lee BS, Aratani N, Zafra JL, Bao N, Lee R, Sung YM, Sun Z, Huang KW, et al. Kinetically blocked stable heptazethrene and octazethrene: closed-shell or open-shell in the ground state? *J Am Chem Soc* 2012, 134:14913–14922.
33. Kamada K, Fuku-en S-I, Minamide S, Ohta K, Kishi R, Nakano M, Matsuzaki M, Okamoto H, Higashikawa H, Inoue K, et al. Impact of diradical character on two-photon absorption: bis(acridine) dimers synthesized from an allenic precursor. *J Am Chem Soc* 2013, 135:232–241.
34. Sun Z, Lee S, Park KH, Zhu X, Zhang W, Zheng B, Hu P, Zeng Z, Das S, Li Y, et al. Dibenzo-heptazethrene isomers with different biradical characters: an exercise of Clar's aromatic sextet rule in singlet biradicaloids. *J Am Chem Soc* 2013, 135:18229–18236.
35. Das S, Lee S, Son M, Zhu X, Zhang W, Zheng B, Hu P, Zeng Z, Sun Z, Zeng W, et al. Para-quinodimethane-bridged perylene dimers and pericondensed quaterrylenes: the effect of the fusion mode on the ground states and physical properties. *Chem-Eur J* 2014, 20:11410–11420.
36. Kishida H, Hibino K, Nakamura A, Kato D, Abe J. Third-order nonlinear optical properties of a  $\pi$ -conjugated biradical molecule investigated by third-harmonic generation spectroscopy. *Thin Solid Films* 2010, 519:1028–1030.
37. Takauji K, Suizu R, Awaga K, Kishida H, Nakamura A. Third-order nonlinear optical properties and electroabsorption spectra of an organic biradical, [Naphtho[2,1-d:6,5-d']bis([1,2,3]dithiazole)]. *J Phys Chem C* 2014, 118:4303–4308.
38. Hayes EF, Siu AKQ. Electronic structure of the open forms of three-membered rings. *J Am Chem Soc* 1971, 93:2090–2091.
39. Heisenberg W. Zur theorie des ferromagnetismus. *Z Phys* 1928, 49:619–636.
40. Nakano M, Minami T, Fukui H, Kishi R, Shigeta Y, Champagne B. Full configuration interaction calculations of the second hyperpolarizabilities of the H<sub>4</sub> model compound: summation-over-states analysis and interplay with diradical characters. *J Chem Phys* 2012, 136:024315.
41. Lopez X, Piris M, Nakano M, Champagne B. Natural orbital functional calculations of molecular polarizabilities and second hyperpolarizabilities. The hydrogen molecule as a test case. *J Phys B: Mol Opt Phys* 2014, 47:015101.
42. Kishi R, Bonness S, Yoneda K, Takahashi H, Nakano M, Botek E, Champagne B, Kubo T, Kamada K, Ohta K, et al. Long-range corrected density functional theory study on static second hyperpolarizabilities of singlet diradical systems. *J Chem Phys* 2010, 132:094107.
43. Nakano M, Minami T, Fukui H, Yoneda K, Shigeta Y, Kishi R, Champagne B, Botek E. Approximate spin-projected spin-unrestricted density functional theory method: application to the diradical character dependences of the (hyper)polarizabilities in *p*-quinodimethane models. *Chem Phys Lett* 2010, 501:140–145.
44. Bonness S, Fukui H, Yoneda K, Kishi R, Champagne B, Botek E, Nakano M. Theoretical investigation on the second hyperpolarizabilities of open-shell singlet systems by spin-unrestricted density functional theory with long-range correction: range separating parameter dependence. *Chem Phys Lett* 2010, 493:195–199.



45. de Wergifosse M, Wautelet F, Champagne B, Kishi R, Fukuda K, Matsui H, Nakano M. Challenging compounds for calculating hyperpolarizabilities: *p*-quinodimethane derivatives. *J Phys Chem A* 2013, 117:4709–4715.
46. de Wergifosse M, Liégeois V, Champagne B. Evaluation of the molecular static and dynamic first hyperpolarizabilities. *Int J Quantum Chem* 2014, 114:900–910.
47. Nakano M, Fukui H, Minami T, Yoneda K, Shigeta Y, Kishi R, Champagne B, Botek E, Kubo T, Ohta K, et al. (Hyper)polarizability density analysis for open-shell molecular systems based on natural orbitals and occupation numbers. *Theoret Chem Acc* 2011, 130:711–724; *erratum* 130: 725.
48. Clar E. *Polycyclic Hydrocarbons*. London: Academic Press; 1964.
49. Yoneda K, Nakano M, Fukui H, Minami T, Shigeta Y, Kubo T, Botek E, Champagne B. Open-shell characters and second hyperpolarizabilities of one-dimensional graphene nanoflakes composed of trigonal graphene units. *ChemPhysChem* 2011, 12:1697–1707.
50. Yoneda K, Nakano M, Fukuda K, Matsui H, Takamuku S, Hirotsaki Y, Kubo T, Kamada K, Champagne B. Third-order nonlinear optical properties of one-dimensional open-shell molecular aggregates composed of phenalenyl radicals. *Chem-Eur J* 2014, 35:11129–11136.